~~TABLE V~~
~~CALIBRATION RESIDUES, RMS PER POINT~~

~~Calibration type~~	~~Source fixtures~~	~~Source type~~ ~~Dipole approx~~	~~Concentric~~
~~(default)~~	~~No~~	~~0.54%~~	~~0.52%~~
	~~Yes~~	~~0.76%~~	~~1.16%~~
~~Concentric~~	~~No~~	~~20.8%~~	~~0.71%~~
	~~Yes~~	~~36.6%~~	~~1.89%~~

TABLE V
CALIBRATION RESIDUES, RMS PER POINT

Calibration type	Source fixtures	Source type Dipole approx	Concentric
(default)	No	0.54%	0.52%
	Yes	0.76%	1.16%
Concentric	No	20.8%	0.71%
	Yes	36.6%	1.89%

I. CALIBRATION PROCEDURES

Calibration optimization is via Matlab `lsqnonlin`. Depending on the test data, and the result calibration desired, we need to restrict the optimization in configurable ways. Control of the optimization is implemented by the bounds specified on the state. An optimization variable is initialized to a desired value, and then forced to not change by limiting the bounds to that value. Which values are "frozen" in this way is configured as needed, without any change in the optimization state space or objective function.

A. Initial values

Optimization will not converge, or will be unreasonably slow, if the initial values are "too far off". This difficulty is vaguely defined, and in practice a certain amount of trial and error (and head-scratching) can be expected. When available, the best initial value is a previous calibration result. If there is a change in the setup then it is worthwhile manually modifying an old calibration to approximate the expected new calibration.

Some initial values are non-critical. Coil formulas or magnetic simulations could be used to predict the gain of the source and sensor. While useful for coil design, it is not needed for the calibration optimization. If the coil arrangement is very roughly concentric and orthogonal, and gain is not too far from 1, then it will often work well to initialize with $\boldsymbol{L} = 0, \boldsymbol{M} = \boldsymbol{I}$.

The most critical initial state is the fixture transforms, since these affect the sign and gross rotation of the predicted coupling $\tilde{\boldsymbol{C}}$. It is easy to get it wrong when attempting to visualize and numerically represent the 3DOF rotation of a setup that includes large fixture rotations.

B. Stepwise optimization

Stepwise optimization, gradually increasing the optimization state space, greatly helps convergence when initial values are poorly known. In practice it works well to use a rough guess for initial values, then first optimize the fixture transforms to find out which way is up, then add sensor moments ${}^{se}\boldsymbol{M}$, and then finally proceed to a full optimization. If optimization fails to converge to a reasonable residual, especially if there is unexpected asymmetry between source coils or sensor coils, check for hardware faults such as sign inversion on source or sensor signal paths.

C. Data degrees of freedom vs. fixture transforms

Data collection is time-consuming, and optimization runtime increases with the input data, so we wish to make preliminary calibrations using reduced data. It is particularly convenient to initially omit fixture motions since these are manual. But when some degrees of freedom are not exercised in the calibration motion pattern, then it is impossible to uniquely identify all of the fixture transform variables, so some must be frozen. The source fixture ${}^{so}\boldsymbol{F}$ cannot be determined without source motion ${}^{so}\boldsymbol{J}$, nor can ${}^{se}\boldsymbol{F}$ be fully determined without ${}^{se}\boldsymbol{J}$. These underdefined fixture transforms do not affect the pose solution since the $\boldsymbol{F}$ only exist to absorb unknowns in the calibration setup.

D. Calibration residue

Table V shows the calibration residue for the various calibrations ~~above~~in the main paper. This is a measure of the quality of fit between the calibration data our chosen $\tilde{\boldsymbol{c}}(\ldots)$, and roughly predicts the attainable measurement accuracy. We can easily see that the (non-concentric) dipole-approximating source performs very badly with a concentric calibration, that adding source fixture motion is going to degrade accuracy, and that even with the concentric source it is useful to use non-concentric calibration.

However, this residue is over coupling matrices, and the pose solution's sensitivity to coupling error varies according to the specific geometry of the test pose. If the magnetic configuration is unfavorable then the pose error is magnified[1]. This likely explains why pose solution for the dipole-approximating source failed to converge when source fixture motion was present, even though the residual is smaller than for the concentric source. There is no single answer to what an acceptable calibration residue is, but the measurement linearity is unlikely to be better than the calibration residue, and changes in $\tilde{\boldsymbol{c}}(\ldots)$ which reduce the residue usually result in higher measurement accuracy.

II. CALIBRATION STAGE

The small scale that we are targeting in the ILEMT microsurgical application is particularly demanding for the calibration stage. The accuracy as a fraction of the source to sensor distance is similar to other EMTs, but the workspace is smaller, so the absolute accuracy required for calibration is also more demanding. To characterize an accuracy of 200 µm we would ideally have a ground truth position accuracy of 20—70 µm. Expressed as an angular error at 200 mm, this is 100—350 microradians, or 0.006—0.020 degrees. (This is not quite achieved, see §B below.)

Given the primary concern for sensor position error (compared to sensor rotation), the accuracy of the source rotation fixture is particularly important, since source rotation error is converted to sensor position error by the moment of the source to sensor radius.

The source and sensor fixtures are machined to be orthogonal

and to have a common origin between their rotational axes. Beyond that, positioning the actuated R_z axis coincident with the sensor fixture coordinates is the only precision mechanical alignment required. This is done by nulling the reading on a mechanical dial test indicator as the R_z axis is moved. The indicator reads the motion of a cylinder mounted in place of the sensor.

While it is crucial that the source and sensor fixtures each have a single center of rotation (defining the that fixture's origin), the fixture transforms (§V.D) permit us to leave ill-defined the mechanical relation between the source and sensor and their fixtures. These arbitrary (but fixed) unknowns are solved for by the calibration optimization.

A. Workspace and degrees of freedom

The stage described cannot access the full hemispherical workspace so that it can be calibrated and tested, and while we do exercise all of the source and sensor rotations (unlike common practice), we do not systematically explore the full 6DOF pose space. As well as not being something that can be done using this sort of positioning hardware, the size of the 6DOF space is daunting in the number of poses that need to be measured.

The limitation to 100mm cube is a hardware constraint, there is no reason why a larger range stage could not be used. Note that EM trackers do not have any hard limit on the operating range, but a practical limit is created by noise that increases as r^4. There would still be mechanical challenges in covering a full hemisphere workspace so far as supporting source and sensor without collisions. Being able to rotate the source is useful for getting all around access because you would not need to access a full hemisphere, but the angular accuracy required is quite high. While also desirable, getting arbitrary 3DOF angular motion at the sensor with magnetic compatibility would also be hard.

B. Uncertainty analysis

The components are Parker Daedal 806004CT (z axis), 310062AT (x, y axes), and 20801RT (R_z axis). These are driven by microstepping motors with optical encoder feedback. To avoid backlash we always approach from the same direction, if necessary crossing the setpoint and backing up. Computing from the component specifications and as-built fixture measurements, the stage pose uncertainty $u(\boldsymbol{P}_{\text{stage}})$ is 118 µm and 2.9 mrad. But the magnetic isolation pole has a large moment arm (0.7 m) converting any off-axis stage $R_x R_y$ motion into XY position error. Inadvertent rotation is a large concern for any such system that uses distance-based magnetic isolation from a metallic positioner, whether it is a motion stage, a robot arm or CMM.

Unfortunately, the incidental off-axis rotation is not specified for the components used. We measured on-axis and off-axis deviations using indicators, granite straightedge, square, and gauge blocks. Combining specifications and measurements (whichever is larger) gave a 246-µm uncertainty, large enough to significantly worsen the uncertainty of some the EMT configurations tested here. We compensated ${}^{st}\boldsymbol{J}$ (section V.D) by adding the measured stage errors, interpolated from lookup tables. With a fairly conservative assumption that this compensation is 75% effective, the uncertainty then becomes 107 µm, which has little effect on the combined uncertainty in Table II.

See `calibration/stage_uncertainty.xlsx` in the `ilemt_papers` repository for the detailed uncertainty calculation.

III. Magnetic Error in the Test Setup

Any magnetic or highly conductive material (mainly metal) must be excluded from the test setup since this is another source of systematic error. As with stage error, this increases the true error $\boldsymbol{E}(\tilde{\boldsymbol{P}})$ seen in other magnetic environments, yet may go undetected by the calibration error $\tilde{\boldsymbol{E}}(\tilde{\boldsymbol{P}})$. Avoiding metal is difficult because standard positioning devices such as stages and robot arms almost invariably contain a considerable amount of metal. ~~Fortunately, any metallic interference drops as r^6, so~~

Fortunately, any metallic interference drops rapidly with distance. The dipole field of the source drops as r^{-3} of the source-to-metal distance, and the metal creates an interfering field proportional to this when must then reach the sensor. If the metal effect could also be modelled as a dipole then the disturbance would decrease as r^{-6}, but empirically we have found the interference to be unmeasurable well before this asymptote is reached. That is, to have an effect the metal must be large enough that it can't be approximated as a dipole. Using a more realistic r^{-4}, if the closest interferer is at 3.2x the source/sensor distance, then the interference will be reduced by ~~1000~~100, which can usually be neglected.

Metallic interference is greatest when the interferer is near the source or sensor, or between them, so this should be avoided. A way to test for the presence of magnetic interference is to attach the source and sensor to a handheld bar and move this about the workspace, finding the distance from each component that causes a detectable change in output.

For 3D translation and a single rotation axis, magnetic isolation can be achieved by placing the sensor on a nonmetal pole extending away from the large metal components in the positioning stage [2][3][4]. We achieve a separation greater than 400 mm between the sensor and metal objects by placing the sensor on a fiberglass pole, but this in itself only permits rotation (R_z) about a single axis. The extra rotations are achieved using the manual source and sensor fixtures.

We found that the black granite is slightly magnetic, so we raise the source fixture above the surface plate. The pink granite plate (Starrett) in the source fixture does not have any detectable magnetic effect. The sensor fixture allows any sensor axis to be aligned with the stage R_z, permitting automated testing on all axes, while the source fixture only supports certain 90º rotations.

IV. Effect of Tracker Drift

As with most measurement devices, it is common for EMTs to show some degree of drift, a relatively slow spurious change in the measurement over time. Of course, time instability must be accounted for in considering the accuracy of any tracker. But this work does not address minimizing the drift of tracker hardware. The present concern for calibration procedures is that the calibration data collection takes a considerable amount of time. If there is any time-dependent error this will undermine the calibration process, so it is necessary for drift to be well less than the desired calibration accuracy. The tested ILEMT tracker (§VIII.E) shows noticeable warmup drift related to temperature rise in the source (Figure 1.) A warmup of 120 minutes is sufficient for the position to stabilize.

References

[1] O. Talcoth and T. Rylander, "Optimization of sensor positions in magnetic tracking," *Chalmers Univ. Technol. Tech. Rep.*, no. R015/2011, pp. 1–30, 2011, [Online]. Available: http://publications.lib.chalmers.se/records/fulltext/149466.pdf.

[2] D. D. Frantz, A. D. Wiles, S. E. Leis, and S. R. Kirsch, "Accuracy assessment protocols for electromagnetic tracking systems," *Phys. Med. Biol.*, vol. 48, no. 14, pp. 2241–2251, Jul. 2003, doi: 10.1088/0031-9155/48/14/314.

[3] M. Schneider and C. Stevens, "Development and testing of a new magnetic-tracking device for image guidance," in *Medical Imaging 2007: Visualization and Image-Guided Procedures*, Mar. 2007, vol. 6505, pp. 65090I-65090I–11, doi: 10.1117/12.713249.

[4] C. Nafis, V. Jensen, L. Beauregard, and P. Anderson, "Method for estimating dynamic EM tracking accuracy of surgical navigation tools," in *Proc.SPIE*, Mar. 2006, vol. 6141, p. 61410K, doi: 10.1117/12.653448.

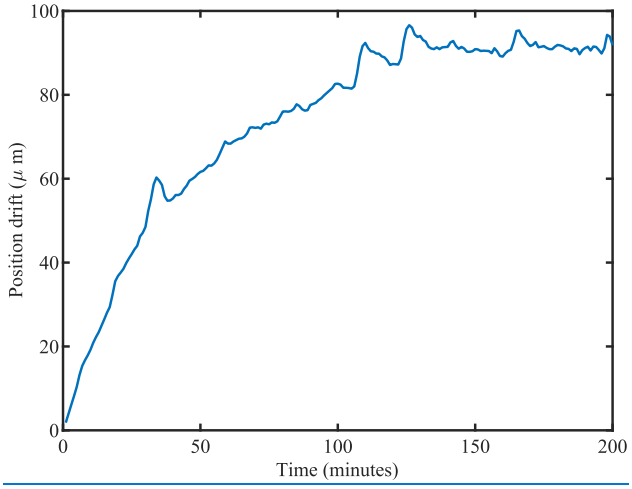

Figure 1: Warmup position drift of the tested tracker hardware (ILEMT) when using the concentric source. Calibration measurements should be made after the position has stabilized.